Eur. Phys. J. A **23**, 249–256 (2005)
DOI 10.1140/epja/i2004-10089-5

THE EUROPEAN PHYSICAL JOURNAL A

Survival probabilities of superheavy nuclei based on recent predictions of nuclear properties

A.S. Zubov[1,2], G.G. Adamian[2,3], N.V. Antonenko[2,a], S.P. Ivanova[2], and W. Scheid[1]

[1] Institut für Theoretische Physik der Justus-Liebig-Universität, D-35392 Giessen, Germany
[2] Joint Institute for Nuclear Research, 141980 Dubna, Russia
[3] Institute of Nuclear Physics, Tashkent 702132, Uzbekistan

Received: 8 July 2004 / Revised version: 29 September 2004 /
Published online: 13 December 2004 –
Communicated by V.V. Anisovich

Abstract. By using the statistical model and recent theoretical predictions of nuclear properties, survival probabilities of superheavy nuclei with respect to the xn evaporation channel ($x = 1$–4) are calculated. Level densities of the Fermi-gas model and of a model with collective enhancement are used. The survival probabilities and the fusion cross-sections calculated within the dinuclear system model are applied to obtain excitation functions of No isotopes in the reactions ^{48}Ca + ^{204,206,208}Pb and production cross-sections of superheavy nuclei with $Z > 102$ in cold and hot fusion reactions. The results are in a good agreement with available experimental data.

PACS. 25.70.Jj Fusion and fusion-fission reactions – 24.10.-i Nuclear-reaction models and methods – 24.60.-k Statistical theory and fluctuations – 24.90.+d Other topics in nuclear reactions: general

1 Introduction

The synthesis of superheavy nuclei in cold- and hot-fusion reactions is an actual interesting field of present-day nuclear physics. The experimental studies of produced isotopes stimulate more precise theoretical description of their properties. New theoretical predictions of the properties of superheavy nuclei have been achieved in refs. [1–4]. They can be used for a more precise calculation of the evaporation residue cross-sections for the production of superheavy elements. At centre-of-mass kinetic energy $E_{\rm c.m.}$ these cross-sections are given for small contributing angular momenta as [5–8]

$$\sigma_{\rm ER}(E_{\rm c.m.}) \approx \sigma_c(E_{\rm c.m.})P_{\rm CN}(E_{\rm c.m.}, J=0) \times W_{\rm sur}(E_{\rm c.m.}, J=0). \quad (1)$$

They depend on the capture cross-section σ_c describing the transition of the colliding nuclei over the entrance (Coulomb) barrier, on the probability $P_{\rm CN}$ of the compound nucleus formation after the capture, and on the survival probability $W_{\rm sur}$ of the excited nucleus. The probability of complete fusion $P_{\rm CN}(E_{\rm c.m.}, J)$, describing the competition between the complete fusion and quasifission, can be calculated within the dinuclear system (DNS) model [5–8]. This model assumes that the compound nucleus is reached by a series of transfers of nucleons or small clusters from the light nucleus to the heavier one in a touching configuration. The dynamics of fusion is considered as a diffusion of the DNS in the mass asymmetry, defined by $\eta = (A_1 - A_2)/(A_1 + A_2)$ (A_1 and A_2 are the mass numbers of the DNS nuclei). The probability $W_{\rm sur}$ determines the survival of the excited compound nucleus and describes the competition between particle evaporation and fission of the compound nucleus. It is considered now as one of the crucial factors in producing heavy and superheavy elements.

Since the calculations of σ_c and $P_{\rm CN}$ in eq. (1) are performed in ref. [8], we use the values presented there and focus on the treatment of $W_{\rm sur}$ in the present paper. In refs. [9,10] we analyzed the survival probabilities of superheavy nuclei with the theoretical predictions of nuclear properties [11–13]. Here, we use the recent predictions [1,2,4] and extend the analysis to the xn evaporation channels ($x \geq 1$). The Fermi-gas model and the model with collective enhancement are applied to the calculation of level densities. Different ways for including the energy dependence of shell effects are considered.

In sect. 2 we give a survey over the survival probability. The calculation of level density with the Fermi-gas model and a model with collective enhancement is discussed in sect. 3. In sect. 4 we present the results for the production of No isotopes, of isotopes with $Z = 103$–109 produced in ^{208}Pb- and ^{209}Bi-based reactions and of the isotopes with $Z = 116$ produced in actinide-based reactions.

[a] e-mail: antonenk@thsun1.jinr.ru

2 Survival probability

The survival probability [14,15] under the evaporation of a certain sequence s of x particles is defined as

$$W_{\rm sur}(E^*_{\rm CN},J) \approx P_s(E^*_{\rm CN},J)\prod_{i_s=1}^{x}\frac{\Gamma_i(E^*_{i_s},J_{i_s})}{\Gamma_t(E^*_{i_s},J_{i_s})}. \quad (2)$$

Here, i_s, P_s, $E^*_{i_s}$ and J_{i_s} are the index of the evaporation step, the probability of realization of the channel s at the initial excitation energy $E^*_{\rm CN}$ of the compound nucleus, the mean values of excitation energy and angular momentum, respectively. At the first step $i_s = 1_s$, $E^*_{1_s} = E^*_{\rm CN}$ and $J_{1_s} = J$. The total width Γ_t for compound nucleus decay is the sum of partial widths of particle evaporation Γ_i, γ-emission Γ_γ and fission Γ_f. In superheavy nuclei with $Z \geq 102$ at considered excitation energies ($E^*_{\rm CN} \geq$ 9–10 MeV, *i.e.* larger than neutron separation energy) the emission of γ-rays and charged particles are much less probable than the neutron emission. The emission of charged particles is suppressed by the large Coulomb barrier and the emission of γ-rays plays only role at smaller $E^*_{\rm CN}$. Under these circumstances we set $\Gamma_i \approx \Gamma_n$ and $\Gamma_t \approx \Gamma_n + \Gamma_f$. Therefore, the survival probability $W_{\rm sur}(E^*_{\rm CN},J)$ reflects the competition between neutron evaporation and fission of the excited compound nucleus. Since in the considered nuclei $\Gamma_n \ll \Gamma_f$, we can write the survival probability in the case of the evaporation of x neutrons [14,15]

$$W_{\rm sur}(E^*_{\rm CN},J) \approx P_{xn}(E^*_{\rm CN},J)\prod_{i=1}^{x}\frac{\Gamma_n(E^*_i,J_i)}{\Gamma_n(E^*_i,J_i)+\Gamma_f(E^*_i,J_i)}$$
$$\approx P_{xn}(E^*_{\rm CN},J)\prod_{i=1}^{x}\frac{\Gamma_n(E^*_i,J_i)}{\Gamma_f(E^*_i,J_i)}, \quad (3)$$

where P_{xn} is the probability of realization of an xn channel at a given $E^*_{\rm CN}$ and J.

In the case of the emission of x neutrons ($x > 1$) we use the well known formula P_{xn}=$P(x+1) - P(x)$ [16,17], where the function

$$P(x) = 1 - \exp[\Delta_x/\overline{T}]\left(1 + \sum_{i=1}^{2x-3}\frac{(\Delta_i/\overline{T})}{i!}\right) \quad (4)$$

is the probability that at a given $E^*_{\rm CN}$ not more than x neutrons are evaporated. Here, $\Delta_i = E^*_{\rm CN} - \sum_{k=1}^{i} B_n(k)$, $B_n(k)$ is the separation energy of the k-th evaporated neutron, $\overline{T} = \sqrt{E^*_{\rm CN}/(1.5a_{\rm CN})}$ the average nuclear temperature, which is taken for simplicity constant in (4) during the whole evaporation process, and $a_{\rm CN}$ the level density parameter for the parent compound nucleus. $\overline{T}$ is defined at $E^*_{\rm CN}/1.5$ to take effectively into account the decrease of nuclear temperature in the evaporation process [17]. The uncertainty of the definition of $\overline{T}$ in (4) leads to the shift of the maxima of calculated excitation functions within 2 MeV at the $E^*_{\rm CN}$ considered. If the fission threshold B_f of the final residual nucleus after the emission of x neutrons is less than the neutron separation energy of the same nucleus, we replace $B_n(x+1)$ by B_f in the expression for Δ_{x+1} [17].

In the case of the $1n$ evaporation channel we use the following parameterization [14,15]

$$P_{1n}(E^*_{\rm CN}) = \exp[-(E^*_{\rm CN} - B_n - 2T)^2/(2\sigma^2)], \quad (5)$$

which is consistent with our previous calculations of P_{1n} [9,10]. Here, $T = \sqrt{E^*_{\rm CN}/a_{\rm CN}}$ is the temperature of compound nucleus and $\sigma = 2.5$ MeV. Note that the direct application of (4) to the $1n$ evaporation channel leads to a P_{1n}, which is smaller by a factor of about 1.3.

The decay width of channel i is given in terms of the probability $R_{{\rm CN}_i}$ of this process as [14,15,18–22]

$$\Gamma_i = \frac{R_{{\rm CN}_i}}{2\pi\rho(E^*_{\rm CN},J)}. \quad (6)$$

The probability of evaporation of particle j (neutron, proton, α-particle)

$$R_{{\rm CN}_j}(E^*_{\rm CN},J) = \sum_{J_d}\int_0^{E^*_{\rm CN}-B_j} {\rm d}\epsilon\rho_d(E^*_{\rm CN}-B_j-\epsilon,J_d)$$
$$\times \sum_{S=|J_d-s|}^{J_d+s}\sum_{l=|J-S|}^{J+S} T_{jl}(\epsilon) \quad (7)$$

can be calculated by using the separation energy B_j of particle j with spin s and the level density $\rho_d(E^*_{\rm CN}-B_j-\epsilon,J_d)$ of the daughter nucleus. The transmission coefficient $T_{jl}(\epsilon)$ through the barrier is calculated by using an optical model potential [18].

The fission probability in the case of an one-hump barrier of height $B_f(E^*_{\rm CN})$ and curvature determined by $\hbar\omega$ is given as

$$R_{{\rm CN}_f}(E^*_{\rm CN},J) =$$
$$\int_0^{E^*_{\rm CN}-B_f(E^*_{\rm CN})}\frac{\rho_f(E^*_{\rm CN}-B_f(E^*_{\rm CN})-\epsilon){\rm d}\epsilon}{1+\exp[2\pi(\epsilon+B_f(E^*_{\rm CN})-E^*_{\rm CN})/(\hbar\omega)]}, \quad (8)$$

where $\rho_f(E^*_{\rm CN} - B_f(E^*_{\rm CN}) - \epsilon)$ is the level density at the saddle point. For all the nuclei considered, we take $\hbar\omega = 2.2$ MeV that is slightly larger than 1.0–1.5 MeV in the actinides because the fission barrier becomes thinner in accordance to the calculations in ref. [13]. The variation of $\hbar\omega$ within 1.0 MeV has a very weak influence on the value of $R_{{\rm CN}_f}$ because at considered excitation energies the fission occurs above the barrier. Thus, in order to find $W_{\rm sur}$, we have to fix the method of the calculation of the level densities, and to determine the fission barriers and B_n.

3 Calculation of the level density

3.1 Fermi-gas model

In the simplest way the level density is calculated with the Fermi-gas model [21] as

$$\rho(E^*_{\rm CN},J)=\frac{2J+1}{24\sqrt{2}\sigma^3 a^{1/4}(E^*_{\rm CN}-\delta)^{5/4}} \times\exp\left\{2\sqrt{a(E^*_{\rm CN}-\delta)}-\frac{(J+1/2)^2}{2\sigma^2}\right\} \quad (9)$$

with $\sigma^2=6\overline{m^2}\sqrt{a(E^*_{\rm CN}-\delta)}/\pi^2$. The pairing correction δ is set $\delta=0.7\approx 12/\sqrt{A}$, 0 and -0.7 MeV for even-even, odd, and odd-odd nuclei, respectively. The level density parameter a is proportional to the density of single-particle states at the Fermi surface. The average projection of the angular momentum of these states is estimated as $\overline{m^2}\approx 0.24A^{2/3}$. In the calculations with (9) we take $a=A/10$ MeV^{-1} for all considered nuclei with $Z\geq 102$. In the level density ρ_f on the fission barrier we set $a_f=1.02a$, which is smaller than $a_f/a=1.1$ used in refs. [9,10] for the $1n$ evaporation channel. For the analysis of (2–4)n evaporation channels this value is more appropriate due to a stronger damping of shell corrections at higher excitations energies. The value of a_f/a is related to the rate of the change of nuclear structure from the ground state to the saddle point [17]. Since the absolute value of the shell corrections at ground states in ref. [2] is smaller than in refs. [11,12], we require a smaller value of a_f/a in the present paper. The variation of the parameters a and a_f/a with the Γ_n/Γ_f ratio was considered in ref. [10]. For small excitation energies $E^*_{\rm CN}<U_x=2.2$ MeV we use the model with constant temperature T [22].

The fission barrier B_f has the liquid-drop and microscopical parts, $B_f^{\rm LD}$ and $B_f^{\rm M}$, respectively. The liquid-drop part is calculated as in ref. [23] for all considered nuclei except for the elements with $Z=103$–105. For these nuclei we set $B_f^{\rm LD}=1$ MeV. The value $B_f^{\rm M}=\delta W^A_{\rm sd}-\delta W^A_{\rm gr}$ is related to the shell correction $\delta W^A_{\rm gr}$ of the nucleus with mass number A at the ground state and the shell correction $\delta W^A_{\rm sd}$ at the saddle point. Usually, one neglects the shell correction at the saddle point, $\delta W^A_{\rm sd}\approx 0$ [24]. Thus, $B_f^{\rm M}=B_f^{\rm M}(E^*_{\rm CN}=0)\approx|\delta W^A_{\rm gr}(E^*_{\rm CN}=0)|$. The same procedure of fixing the fission barrier was used in refs. [7–10] for the calculations of $W_{\rm sur}$ with the predictions of refs. [11,12]. Among the values, which are necessary for calculating Γ_f, refs. [11,12] supply only $\delta W^A_{\rm gr}$. Besides $\delta W^A_{\rm gr}$ refs. [2,3] give the static fission barrier. To be consistent with our previous calculations which apply the nuclear properties of refs. [11,12], and being aware that the characteristics of the nuclear ground state are usually more reliable for superheavy nuclei [25], we use the procedure mentioned above for the determination of $B_f^{\rm M}$.

In the Fermi-gas model the dependence of the shell effects on the nuclear excitation is effectively introduced via the dependence of B_f on $E^*_{\rm CN}$ with damping of the microscopical part

$$B_f(E^*_{\rm CN})=B_f^{\rm LD}+B_f^{\rm M}(E^*_{\rm CN}=0)\exp[-E^*_{\rm CN}/E_{\rm D}]. \quad (10)$$

In the calculations, we use the following expression for $E_{\rm D}$ suggested in ref. [26]:

$$E_{\rm D}=\alpha_0 A^{4/3}/a\ , \quad (11)$$

where $\alpha_0=0.4$. Another method to take into account the damping of the shell effects is using an energy-dependent level density parameter [10], which is applied in the model with collective enhancement (see next subsection). Both methods are equivalent at an appropriate choice of the damping factors [10].

3.2 Model with collective enhancement

Taking into account the pairing correlations, collective vibrations and rotations of nuclei, we write the level density as [21,22]

$$\rho(E^*_{\rm CN},J)=K_{\rm vib}(E^*_{\rm CN})K_{\rm rot}(E^*_{\rm CN}) \times\frac{2J+1}{24\sqrt{2}\sigma^3_{\rm eff}a^{1/4}(E^*_{\rm CN}-E_c)^{5/4}} \times\exp\left\{2\sqrt{a(E^*_{\rm CN}-E_c)}-\frac{(J+1/2)^2}{2\sigma^2_{\rm eff}}\right\}, \quad (12)$$

where $K_{\rm vib}$ and $K_{\rm rot}$ are coefficients [21] increasing the level density due to collective vibrations and rotations, respectively. The definitions of $K_{\rm vib}$, $K_{\rm rot}$, $\sigma_{\rm eff}$ and of the condensation energy E_c, which decreases the ground state energy of the Fermi-gas by 1–3 MeV due to the correlation interaction in the nuclei considered, are given in refs. [10,21]. Since the dependence of the Γ_n/Γ_f ratios on the quadruple deformation parameters $\beta_2^{\rm gr}$ at the ground state is rather weak for the nuclei considered, as it was shown in ref. [10], we set the same value of $\beta_2^{\rm gr}=0.2$ for all nuclei considered. That is consistent with the results of ref. [2]. The deformation parameter at the saddle point is determined through the deformation parameter at the ground state: $\beta_2^{\rm sd}\approx\beta_2^{\rm gr}+0.2=0.4$. To describe odd-even effects one can use an effective condensation energy $E_{c,\rm eff}=E_c-\delta$. For small excitation energies, the thermodynamical functions for the calculation of the level density can be found by using the superliquid model [21].

In order to take the dependence of the shell effects on $E^*_{\rm CN}$ into account, one can use a level density parameter a depending on excitation energy [21,22] as follows:

$$a=\tilde{a}(A) \times\left[1+\frac{1-\exp\{-(E^*_{\rm CN}-E_c)/E'_{\rm D}\}}{E^*_{\rm CN}-E_c}\delta W^A_{\rm gr}(E^*_{\rm CN}=0)\right], \quad (13)$$

where the asymptotic level density parameter $\tilde{a}(A)$ is set as [22]

$$\tilde{a}(A)=0.114A+0.162A^{2/3}. \quad (14)$$

The damping parameter $E'_{\rm D}$ is determined by eq. (11) with $\alpha_0=0.5$. This choice of α_0 leads to results closest to the results obtained with the Fermi-gas approach described

above. A possible variation of the parameters α_0 and $\tilde{a}(A)$ and its influence on final results are discussed in ref. [10]. In the model with collective enhancement the damping of the shell effects has been already taken into account in the level density parameter. Therefore, a damping factor in the microscopical part of fission barrier is no more required, and

$$B_f = B_f^{\rm LD} + B_f^{\rm M}(E^*_{\rm CN} = 0). \qquad (15)$$

4 Results and discussion

For the calculation of the decay widths we used the statistical code GROGIF [18–20]. Since $\sigma_{\rm ER}$ can be factorized into three factors in (1) with $W_{\rm sur}(E^*_{\rm CN}, J = 0)$ reduced to zero angular momentum [7], the calculations of the survival probability were done for J=0 only. The dependence on J is effectively taken into account in σ_c [7,26]. The factorization (1) holds good if the partial waves with $J < 10$–15 have the largest contributions to the evaporation residue cross-section. The last is true for superheavy nuclei due to the sharp decrease of $W_{\rm sur}$ with increasing J.

The calculations of $W_{\rm sur}$ are carried out in the Fermi-gas model with (9), $a = A/10$ MeV^{-1}, and fission barriers (10) and in the model accounting the collective enhancement of the level density with (12), (13), (14), and fission barriers (15). The recent theoretical predictions for neutron separation energies [1,4] and shell corrections [2] are used. The capture cross-sections σ_c are calculated as in refs. [7,8], where the values of $P_{\rm CN}$ are presented as well.

We calculated the survival probabilities $W_{\rm sur}$ as functions of $E^*_{\rm CN}$ for xn evaporation channels ($x > 1$). Since in ^{208}Pb- and ^{209}Bi-based reactions with excitation energies $E^*_{\rm CN} > 20$ MeV, the capture cross-section σ_c depends weakly on $E^*_{\rm CN}$ and the function $P_{\rm CN}(E^*_{\rm CN})$ is not steep, one can conclude that the positions of the maxima of excitation functions are close to those of the survival probabilities. The energy dependence of $W_{\rm sur}$ is determined by the energy dependencies of the factors $\prod_{i=1}^{x}(\Gamma_n/\Gamma_f)_i$ and P_{xn} in eq. (3). In fig. 1 these two factors and $P_{\rm CN}$ are presented as functions of $E^*_{\rm CN}$ for $2n$ and $3n$ evaporation channels for the compound nucleus ^{262}106 produced in the ^{54}Cr + ^{208}Pb reaction.

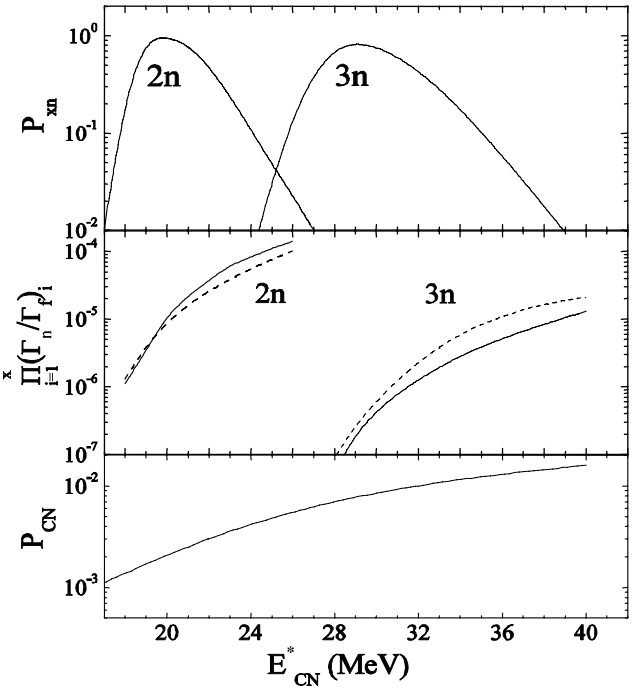

Fig. 1. The calculated P_{xn}, $\prod_{i=1}^{x}(\Gamma_n/\Gamma_f)_i$ and $P_{\rm CN}$ as functions of $E^*_{\rm CN}$ for $2n$ and $3n$ evaporation channels for the compound nucleus ^{262}106. The solid and dashed curves show the results obtained for $\prod_{i=1}^{x}(\Gamma_n/\Gamma_f)_i$ with the Fermi-gas model and with the model accounting a collective enhancement of the level density, respectively.

4.1 Production of nobelium isotopes

Production cross-sections and excitation functions of different isotopes of No have been measured in the reactions ^{48}Ca + ^{204,206,208}Pb in different experiments [27–30]. For these reactions the internal fusion barrier and the quasifission barrier are practically equal to each other. Therefore, the probability of complete fusion $P_{\rm CN}$ is approximately 0.5 and the evaporation residue cross-sections are mainly determined by the survival probabilities for the $2n$, $3n$ and $4n$ evaporation channels. The $1n$ evaporation channel partially lies in the sub-barrier region that is taken into account in the capture cross-section σ_c. For the reactions ^{48}Ca + ^{208}Pb and ^{48}Ca + ^{206}Pb the calculated Coulomb barriers are 171.35 MeV and 171.67 MeV respectively, and the frequencies of inverted oscillators fitting the barriers near their tops result in 2.5 MeV.

The experimental values and the results of our calculations are shown in figs. 2-4. The error bars represent the statistical uncertainties. Comparing the results of various measurements shown in fig. 2, we conclude that the systematic uncertainty in the definition of $\sigma_{\rm ER}$ is up to a factor of 3. The systematic uncertainty in the definition of excitation energy is about 1.7 MeV in ref. [28]. Taking the experimental uncertainties and the differences between various measurements into account, the calculated values of $\sigma_{\rm ER}$ are in a good agreement with the experimental data for the most of evaporation channels, especially near the maxima of excitation functions. The calculated values of $\sigma_{\rm ER}$ in figs. 2-4 were obtained with the same set of parameters for all nobelium isotopes and without a specific modification of $B_f^{\rm LD}$, like in ref. [27].

In the ^{48}Ca + ^{206}Pb reaction (fig. 3) the deviation of the experimental points from the tails of calculated excitation functions on the right-hand side could be partly related to contaminations with heavier isotopes in the ^{206}Pb target. For example, this target contains about 2% of ^{207}Pb. The contribution from the reaction ^{207}Pb(^{48}Ca, $2n$)^{253}No into the experimental evaporation residue cross-section of ^{253}No is about 30 nb at excitation

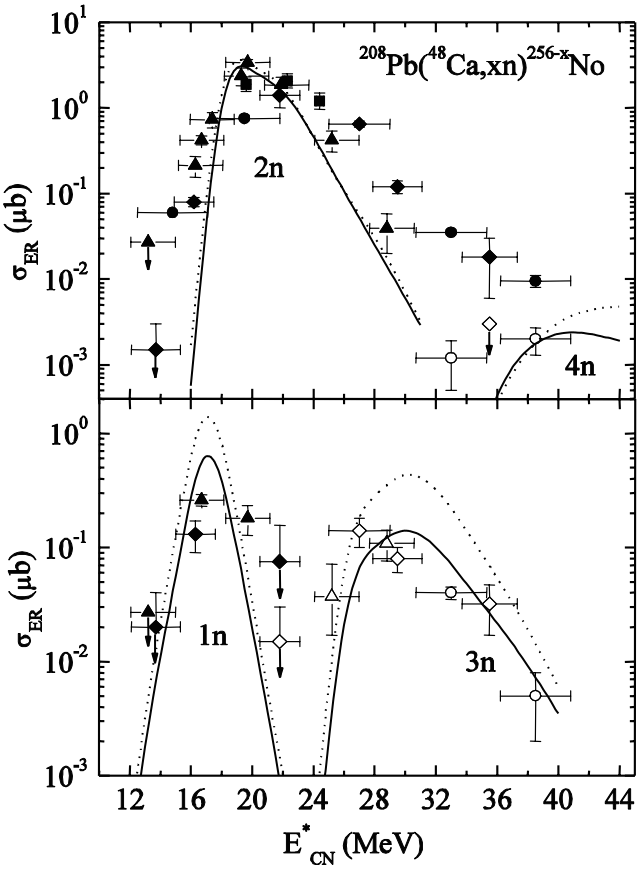

Fig. 2. Measured and calculated excitation functions for xn evaporation channels in the ^{48}Ca + ^{208}Pb reaction. The experimental data from refs. [27–29] and [30] are presented by circles, squares, triangles and diamonds, respectively. The solid symbols correspond to the $1n$ and $2n$ channels. The open symbols correspond to the $3n$ and $4n$ channels. The solid and dashed curves show the results obtained with the Fermi-gas model and with the model accounting a collective enhancement of the level density, respectively.

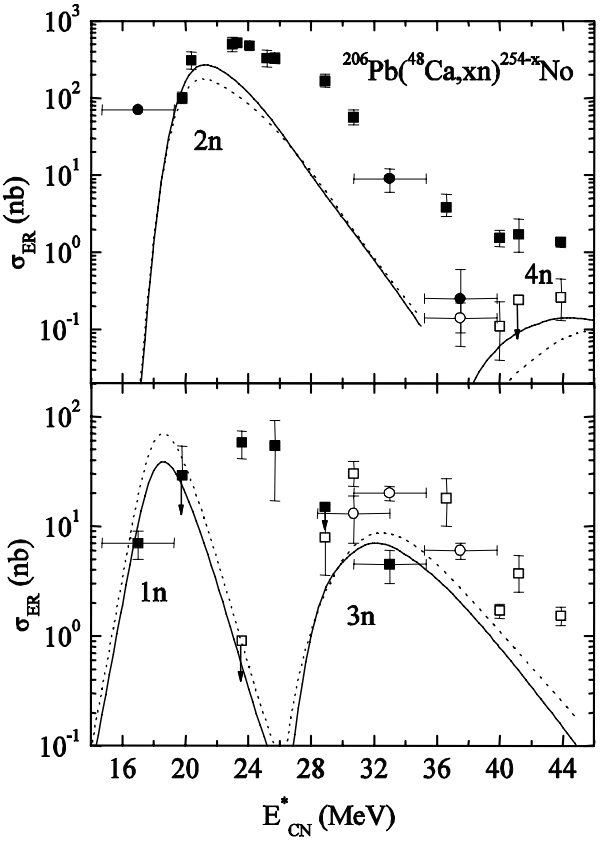

Fig. 3. The same as in fig. 2, but for the reaction ^{48}Ca + ^{206}Pb. The experimental data from refs. [27] and [28] are presented by circles and squares, respectively.

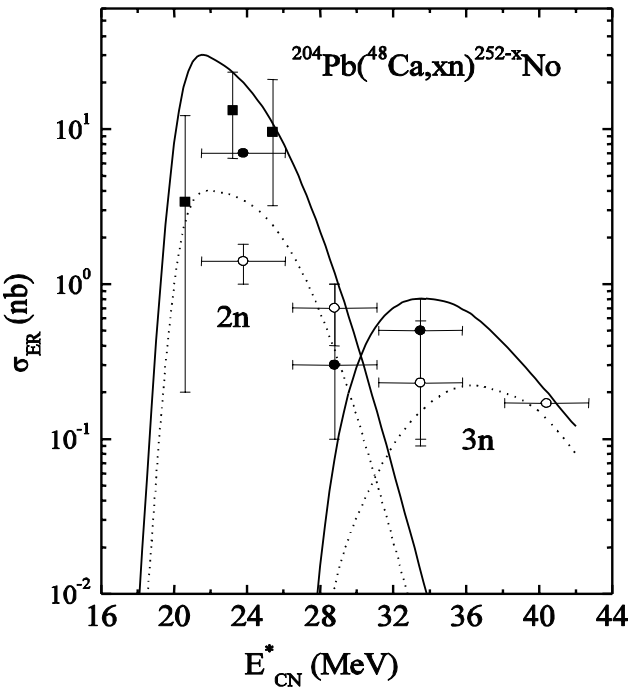

Fig. 4. The same as in fig. 2, but for the reaction ^{48}Ca + ^{204}Pb. The experimental data from refs. [27] and [28] are presented by circles and squares, respectively.

energies of 23–25 MeV. One should note the attempts to regard contributions from target contaminations in experimental studies [28], but it is difficult to make it very precise due to the systematic uncertainties of the measurements of the excitation functions in reactions with different Pb targets.

Since in refs. [27,28] the evaporation residues were identified by the spontaneous fission activity, the spontaneous fission from different states of the same nobelium isotope hinders the resolution of different evaporation channels in some cases. For example, the experimental point shown in fig. 4 by an open circle at $E^*_{\rm CN} = 23.8$ MeV was related to the ^{204}Pb(^{48}Ca, $3n$)^{249}No reaction in ref. [27]. However, one can not exclude that this point belongs to the ^{204}Pb(^{48}Ca, $2n$)^{250}No reaction [27]. For $E^*_{\rm CN} = 20$–26 MeV, the spontaneous fission from two different states of ^{250}No can create two spontaneous fission activities related to the solid and open symbols in fig. 4, respectively.

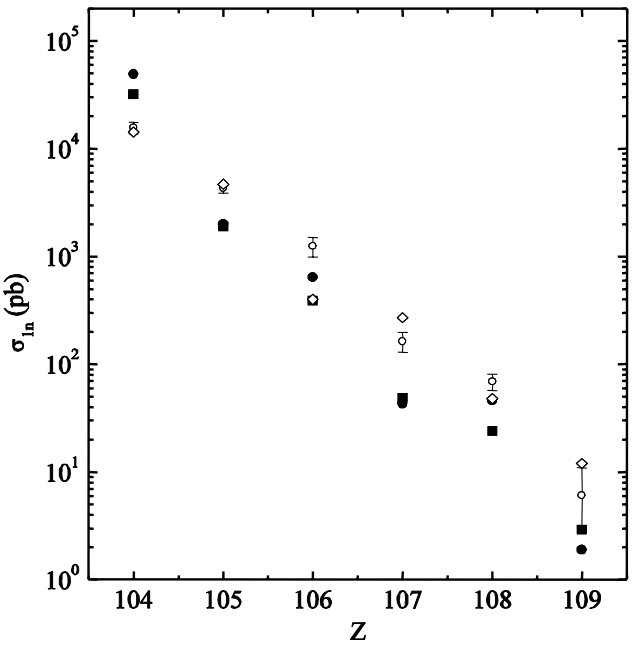

Fig. 5. The evaporation residue cross-sections in the $1n$ evaporation channel for the cold fusion ^{208}Pb- and ^{209}Bi-based reactions leading to the compound nuclei with $Z = 104$–109. The results obtained with the Fermi-gas model and with the model accounting a collective enhancement of the level density are presented by solid squares and circles, respectively. The predictions of nuclear properties of refs. [1,2] are used. The results of ref. [9] obtained with the Fermi-gas model and the predictions of ref. [11] are presented by open diamonds for comparison. The experimental data [31] are given by open circles with error bars.

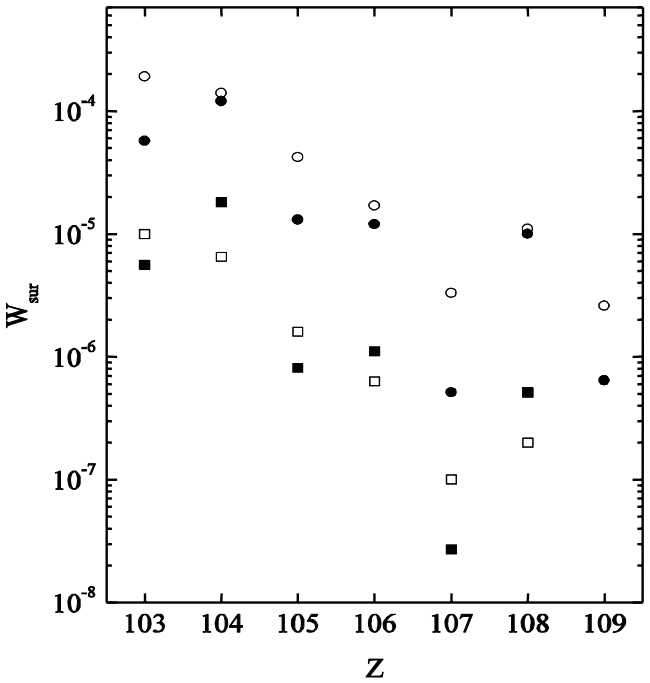

Fig. 6. The calculated maxima of survival probabilities for $2n$ (circles) and $3n$ (squares) evaporation channels as a function of the charge number of the compound nucleus. The open and solid symbols show the results obtained with the Fermi-gas model and with the model accounting a collective enhancement of the level density, respectively.

4.2 Production of isotopes with Z = 103–109 in ^{208}Pb- and ^{209}Bi-based reactions

The measured [31] and calculated evaporation residue cross-sections in the $1n$ evaporation channel for the cold fusion ^{208}Pb- and ^{209}Bi-based reactions leading to compound nuclei with $Z = 104$–109 are shown in fig. 5. The values of excitation energies of each compound nucleus correspond to the maxima of excitation functions [8,31]. The probabilities of complete fusion $P_{\rm CN}$ are taken from ref. [8] for calculating σ_{1n} with eq. (1). The calculations of survival probabilities are carried out with the theoretical predictions of nuclear properties given in refs. [1,2]. From the analysis of fig. 5 one can conclude for the $1n$ evaporation channel that the results for σ_{1n} do not strongly depend on the methods of calculations of the level density; the maximal difference for $Z = 108$ is about a factor of 2. The values of $\sigma_{\rm ER}$ obtained with the predictions of refs. [1,2] are close to those obtained with the structure predictions of ref. [11] for all considered nuclei except for $Z = 107$ and $Z = 109$. The agreement of our results with the experimental data is within a factor of 3, whereas the systematic uncertainty of the experimental cross-sections is within a factor of 2. The strong decrease of $\sigma_{\rm ER}$ with increasing Z is mainly determined by the decrease of the fusion probability $P_{\rm CN}$, as $W_{\rm sur}$ varies much slower from the maximal value 3.1×10^{-4} for ^{258}Rf to the minimal one 7.9×10^{-5} for ^{267}Mt.

The maxima of survival probabilities for the $2n$ and $3n$ evaporation channels for isotopes with $Z = 103$–109 are shown in fig. 6. They were calculated with the structure predictions of refs. [1,2]. The survival probabilities decrease with increasing Z in the considered interval both in $2n$ and $3n$ evaporation channels, except for a local maximum at $Z = 108$, which reflects the approaching to the $N = 162$ shell closure. The results for the $2n$ channel obtained with the Fermi-gas model are close to those obtained with the collective enhancement model for even-even nuclei, but differ up to a factor of 5 for odd nuclei. The values of $W_{\rm sur}$ in the $3n$ channel obtained with the collective enhancement model are larger than those obtained with the Fermi-gas model for even-even nuclei, and smaller for odd nuclei. In the model with collective enhancement the odd-even effects have a stronger influence on the final results, since the level density parameters are energy dependent in this model and the odd-even effects are included in this dependence. Note that the difference between the results obtained with the Fermi-gas and collective enhancement models is not so large if one applies the structure predictions of ref. [11]. For example, one gets a difference of about a factor of 3 for the $2n$ evaporation channel at $Z = 107$.

The evaporated residue cross-sections calculated with the survival probabilities presented in fig. 6 are listed in table 1. The probabilities of complete fusion $P_{\rm CN}$ are taken

Table 1. Experimental [31] $\sigma_{\rm ER}^{\rm exp}$ and theoretical $\sigma_{\rm ER}^{\rm th}$ evaporation residue cross-sections for $2n$ and $3n$ evaporation channels for heavy-ion reactions at the indicated excitation energy $E_{\rm CN}^*$. The results were obtained with the survival probabilities calculated with the Fermi-gas model (fermi) and with the model accounting a collective enhancement (coll).

Reactions	$E_{\rm CN}^*$ (MeV)	$\sigma_{\rm ER}^{\rm th}$ (fermi)	$\sigma_{\rm ER}^{\rm th}$ (coll)	$\sigma_{\rm ER}^{\rm exp}$
^{48}Ca + ^{209}Bi → $^{255}103 + 2n$	20	0.5 μb	0.15 μb	
^{48}Ca + ^{209}Bi → $^{254}103 + 3n$	30.5	25 nb	14 nb	
^{50}Ti + ^{208}Pb → $^{256}104 + 2n$	21.5	44 nb	44 nb	$18.5^{+1.42}_{-1.42}$ nb
^{50}Ti + ^{208}Pb → $^{255}104 + 3n$	29.5	2.3 nb	4.5 nb	$0.993^{+0.21}_{-0.21}$ nb
^{50}Ti + ^{209}Bi → $^{257}105 + 2n$	21.9	1.7 nb	0.6 nb	$2.4^{+0.3}_{-0.3}$ nb
^{50}Ti + ^{209}Bi → $^{256}105 + 3n$	31	150 pb	70 pb	190^{+40}_{-40} pb
^{54}Cr + ^{208}Pb → $^{260}106 + 2n$	22	0.27 nb	0.16 nb	$0.5^{+0.069}_{-0.069}$ nb
^{54}Cr + ^{208}Pb → $^{259}106 + 3n$	32	27 pb	41 pb	10^{+23}_{-8} pb
^{54}Cr + ^{209}Bi → $^{261}107 + 2n$	22	14.5 pb	3 pb	
^{54}Cr + ^{209}Bi → $^{260}107 + 3n$	32	3.2 pb	0.8 pb	
^{58}Fe + ^{208}Pb → $^{264}108 + 2n$	20.5	4.7 pb	5.1 pb	$4.54^{+5.7}_{-2.9}$ pb
^{58}Fe + ^{208}Pb → $^{263}108 + 3n$	32	0.96 pb	1.5 pb	
^{58}Fe + ^{209}Bi → $^{265}109 + 2n$	22	5 pb	1.2 pb	

from ref. [8] in this calculation. The available experimental values of $\sigma_{\rm ER}$ [31] are presented as well. These values are in a good agreement with our results. The differences between the results obtained with the Fermi-gas model and the collective enhancement model correspond to the differences between $W_{\rm sur}$ in fig. 6. The predicted production cross-sections of ^{261}Bh, ^{260}Bh, ^{263}Hs and ^{267}Mt are quite large and favourable for the synthesis of these isotopes in the experiment.

4.3 Production of isotopes of the Z = 116 nucleus in actinide-based reactions

In the hot fusion reactions ^{48}Ca + ^{245,248}Cm the yield of the element 116 is expected for $E_{\rm CN}^* \geq 30$ MeV which corresponds to $E_{\rm c.m.}$ supplying the capture at all relative orientations of the spherical projectile and deformed targets. Let us compare the cross-section σ_{3n} in the reaction ^{48}Ca + ^{245}Cm → $^{290}116 + 3n$ ($P_{\rm CN} = 6 \times 10^{-4}$) at $E_{\rm CN}^* = 30$ MeV with the cross-section σ_{4n} in the reaction ^{48}Ca + ^{248}Cm → $^{292}116 + 4n$ ($P_{\rm CN} = 10^{-4}$) at $E_{\rm CN}^* = 36$ MeV. These cross-sections are maximal at the energies indicated. Due to a smaller Q-value, the $3n$ evaporation channel gets some preference in the ^{48}Ca + ^{245}Cm reaction. For the first reaction we calculate $W_{\rm sur} = 4 \times 10^{-6}$, for the second one $W_{\rm sur} = 3 \times 10^{-6}$. Thus, we get $\sigma_{3n}/\sigma_{4n} \approx 8$. Almost the same ratio was obtained in ref. [32] by using the predictions of nuclear properties of ref. [11]. Thus, with the predictions of ref. [4] one can expect the same isotopic trends in $\sigma_{\rm ER}$ as we found in ref. [32] with the predictions of refs. [11,12,24]. Also we showed for ^{48}Ca-induced hot fusion-evaporation reactions [32] that the actinide targets with smaller neutron excess within certain intervals are more favorable than those with larger neutron excess.

5 Summary

The survival probability of superheavy nuclei is analyzed by using various methods of the calculation of level density and recent theoretical predictions of neutron separation energies and shell corrections from refs. [1,2,4]. Evaporation residue cross-sections were obtained for different superheavy nuclei produced in the reactions ^{48}Ca + ^{204,206,208}Pb and ^{50}Ti, ^{54}Cr, ^{58}Fe + ^{208}Pb, ^{209}Bi. These calculations show that the superheavy nuclei ^{261}Bh, ^{260}Bh, ^{263}Hs and ^{265}Mt could be produced with quite large cross-sections. The calculated and measured values are in a good agreement without any additional adjustments of parameters. The choice of level density parameter a and a_f/a ratio in the Fermi-gas model, asymptotic level densities in the model with collective enhancement and damping in both models is the most crucial for the final results. The impact of this choice on the final results was carried out in ref. [10]. We would stress that the used set of parameters is fixed for all the nuclei considered in this paper and their variation leads to the scale of all calculated evaporation residue cross-sections.

For the $1n$ evaporation channel, the results obtained with various methods of the calculation of the level density and with the theoretical predictions of refs. [1,2] are close to the results applying the theoretical predictions of ref. [11]. For the xn evaporation channels, the two considered methods of the calculation of the level density lead to similar values of $W_{\rm sur}$ for the most nuclei considered. Since the treatment with the Fermi-gas model is simpler and contains a smaller number of parameters, it can be efficiently used for calculating $W_{\rm sur}$.

Taking the nucleus $Z = 116$ as an example, we found the same isotopic trends in $\sigma_{\rm ER}$ for the hot fusion actinide-based reactions with ^{48}Ca beam with using the

predictions of the nuclear properties from refs. [1–4] as it was demonstrated in ref. [32] with the structure predictions of refs. [11,12,24].

A.S.Z. is grateful to DAAD for the support. The supports of VW-Stiftung, DFG, RFBR and Polish-JINR Cooperation Programme are acknowledged.

References

1. O. Parkhomenko, I. Muntian, Z. Patyk, A. Sobiczewski, Acta Phys. Pol. B **34**, 2153 (2003).
2. I. Muntian, S. Hofmann, Z. Patyk, A. Sobiczewski, Acta Phys. Pol. B **34**, 2073 (2003).
3. I. Muntian, Z. Patyk, A. Sobiczewski, Acta Phys. Pol. B **34**, 2141 (2003).
4. I. Muntian, Z. Patyk, A. Sobiczewski, Acta Phys. Pol. B **32**, 691 (2001).
5. N.V. Antonenko, E.A. Cherepanov, A.K. Nasirov, V.B. Permjakov, V.V. Volkov, Phys. Lett. B **319**, 425 (1993); Phys. Rev. C **51**, 2635 (1995).
6. G.G. Adamian, N.V. Antonenko, S.P. Ivanova, W. Scheid, Nucl. Phys. A **646**, 29 (1999).
7. G.G. Adamian, N.V. Antonenko, W. Scheid, V.V. Volkov, Nucl. Phys. A **633**, 409 (1998); Nuovo Cimento A **110**, 1143 (1997).
8. G.G. Adamian, N.V. Antonenko, W. Scheid, Nucl. Phys. A **678**, 24 (2000).
9. G.G. Adamian, N.V. Antonenko, S.P. Ivanova, W. Scheid, Phys. Rev. C **62**, 064303 (2000).
10. A.S. Zubov, G.G. Adamian, N.V. Antonenko, S.P. Ivanova, W. Scheid, Phys. Rev. C **65**, 024308 (2002); Yad. Fiz. **66**, 242 (2003).
11. P. Möller, R. Nix, At. Data Nucl. Data Tables **39**, 213 (1988); LANL Preprint LA-UR-86-3983 (1986).
12. P. Möller, W.D. Myers, W.J. Swiatecki, At. Data Nucl. Data Tables **59**, 185 (1995).
13. R. Smolanczuk, J. Skalski, A. Sobiczewski, Phys. Rev. C **52**, 1871 (1995); R. Smolanczuk, Phys. Rev. C **59**, 2634 (1999).
14. E.A. Cherepanov, A.S. Iljinov, M.V. Mebel, J. Phys. G **9**, 931 (1983).
15. E.A. Cherepanov, in *Proceedings of the International Symposium on In-Beam Nuclear Spectropscopy, Debrecen, Hungary, May 14-18, 1984*, edited by Zs. Dombrádi, T. Féenyes (Akadémiai Kaidóo, Budapest, 1984) p. 499; E.A. Cherepanov, A.S. Iljinov, Nucleonika **25**, 611 (1980); E.A. Cherepanov, Preprint JINR, E7-99-27 (1999).
16. A.S. Zubov, G.G. Adamian, N.V. Antonenko, S.P. Ivanova, W. Scheid, Phys. Rev. C **68**, 014616 (2003)
17. R. Vandenbosch, J.R. Huizenga, *Nuclear Fission* (Academic Press, New York, 1973).
18. J. Gilat, Phys. Rev. C **1**, 1432 (1970).
19. O.V. Grusha *et al.*, Nucl. Phys. A **429**, 313 (1984).
20. O.V. Grusha, S.P. Ivanova, Yu.N. Shubin, VANT, Nuclear Constants **1**, 36 (1987).
21. A.V. Ignatyuk, K.K. Istekov, G.N. Smirenkin, Sov. J. Nucl. Phys. **29**, 875 (1979).
22. A.V. Ignatyuk, *Statistical Properties of Excited Atomic Nuclei* (Energoatomizdat, Moscow, 1983).
23. A.J. Sierk, Phys. Rev. C **33**, 2039 (1986).
24. W.D. Myers, W.J. Swiatecki, Phys. Rev. C **60**, 014606 (1999); Nucl. Phys. A **601**, 141 (1996); Preprint LBL-36803 (1994).
25. A. Sobiczewski, private communication.
26. K.H. Schmidt, W. Morawek, Rep. Prog. Phys. **54**, 949 (1991); K.H. Schmidt *et al.*, in *Proceedings of the Symposium on Physics and Chemistry of Fission, Jülich* (IAEA, Vienna, 1980) p. 409.
27. A.V. Belozerov *et al.*, Eur. Phys. J. A **16**, 447 (2003).
28. Yu.Ts.Oganessian *et al.*, Phys. Rev. C **64**, 054606 (2001).
29. H.W. Gäggeler *et al.*, Nucl. Phys. A **502**, 561 (1989).
30. A.V. Yeremin *et al.*, JINR Rapid Commun. No. 6[92]-98, 21 (1998).
31. S. Hofmann, G. Münzenberg, Rev. Mod. Phys. **72**, 733 (2000); S. Hofmann, Rep. Prog. Phys. **61**, 636 (1998); private communication.
32. G.G. Adamian, N.V. Antonenko, W. Scheid, Phys. Rev. C **69**, 014607 (2004).